

This discussion paper is/has been under review for the journal Climate of the Past (CP).
Please refer to the corresponding final paper in CP if available.

Expansion and diversification of high-latitude radiolarian assemblages in the late Eocene linked to a cooling event in the Southwest Pacific

K. M. Pascher^{1,2}, C. J. Hollis¹, S. M. Bohaty³, G. Cortese¹, and R. M. McKay²

¹GNS Science, P.O. Box 30368, Lower Hutt 5040, New Zealand

²Victoria University Wellington, Antarctic Research Centre, P.O. Box 600, Wellington 6140, New Zealand

³Ocean and Earth Science, National Oceanography Centre Southampton, University of Southampton Waterfront Campus, European Way, Southampton SO14 3ZH, UK

Received: 16 June 2015 – Accepted: 18 June 2015 – Published: 09 July 2015

Correspondence to: K. M. Pascher (k.pascher@gns.cri.nz)

Published by Copernicus Publications on behalf of the European Geosciences Union.

Expansion and diversification of high-latitude radiolarian assemblages

K. M. Pascher et al.

Title Page

Abstract

Introduction

Conclusions

References

Tables

Figures

◀

▶

◀

▶

Back

Close

Full Screen / Esc

Printer-friendly Version

Interactive Discussion

Abstract

The Eocene was characterised by “greenhouse” climate conditions that were gradually terminated by a long-term cooling trend through the middle and late Eocene. This long-term trend was determined by several large-scale climate perturbations that culminated in a shift to “ice-house” climates at the Eocene–Oligocene Transition. Geochemical and micropaleontological proxies suggest that tropical-to-subtropical sea-surface temperatures persisted into the late Eocene in the high-latitude Southwest Pacific Ocean. Here, we present radiolarian microfossil assemblage and foraminiferal oxygen and carbon stable isotope data from Deep Sea Drilling Project (DSDP) Sites 277, 280, 281 and 283 from the middle Eocene to early Oligocene (~40–33 Ma) to identify oceanographic changes in the Southwest Pacific across this major transition in Earth’s climate history. The Middle Eocene Climatic Optimum at ~40 Ma is characterised by a negative shift in foraminiferal oxygen isotope values and a radiolarian assemblage consisting of about 5% of low latitude taxa *Amphicraspedum prolixum* group and *Amphymenium murrayanum*. In the early late Eocene at ~37 Ma, a positive oxygen isotope shift can be correlated to the Priabonian Oxygen Isotope Maximum (PrOM) event – a short-lived cooling event recognized throughout the Southern Ocean. Radiolarian abundance, diversity, and preservation increase during the middle of this event at Site 277 at the same time as diatoms. The PrOM and latest Eocene radiolarian assemblages are characterised by abundant high-latitude taxa. These high-latitude taxa also increase in abundance during the late Eocene and early Oligocene at DSDP Sites 280, 281 and 283 and are associated with very high diatom abundance. We therefore infer a northward expansion of high-latitude radiolarian taxa onto the Campbell Plateau towards the end of the late Eocene. In the early Oligocene (~33 Ma) there is an overall decrease in radiolarian abundance and diversity at Site 277, and diatoms are absent. These data indicate that, once the Tasman Gateway was fully open in the early Oligocene, a frontal system similar to the present day was established, with nutrient-depleted subantarctic

Expansion and diversification of high-latitude radiolarian assemblages

K. M. Pascher et al.

Title Page

Abstract

Introduction

Conclusions

References

Tables

Figures



Back

Close

Full Screen / Esc

Printer-friendly Version

Interactive Discussion



Expansion and diversification of high-latitude radiolarian assemblages

K. M. Pascher et al.

[Title Page](#)

[Abstract](#)

[Introduction](#)

[Conclusions](#)

[References](#)

[Tables](#)

[Figures](#)

[◀](#)

[▶](#)

[◀](#)

[▶](#)

[Back](#)

[Close](#)

[Full Screen / Esc](#)

[Printer-friendly Version](#)

[Interactive Discussion](#)

geochemical proxy data and these paleoecological reconstructions are at odds with the latest generation of ocean circulation and climate modelling simulations (Hollis et al., 2012; Lunt et al., 2012). Even under hyper-greenhouse conditions, the models produce a cyclonic gyre that blocks subtropical waters from penetrating southward beyond 45° S (Huber and Sloan, 2001; Huber et al., 2004). High-latitude warmth also conflicts with evidence for the initiation of Antarctic glaciation in the latest Eocene from both fossil and geochemical proxies (Lazarus and Caulet, 1993; Scher et al., 2014; Barron et al., 2015).

Paleobiogeographic changes in marine biota may help to delineate general climate trends and events. Identifying the initial timing and development of a high-latitude fauna in the Southern Ocean helps to constrain the development of the Southern Ocean frontal systems and, in turn, heat transfer between low and high latitudes. The timing of the establishment of a distinct Southern Ocean surface-water mass is inferred to have occurred within the middle-to-late Eocene interval, triggered by the opening of the Tasman Gateway or changes in carbon cycling (Stickley et al., 2004; Lazarus et al., 2008; Bijl et al., 2013), or abruptly at the E-O transition, associated development of a proto-Antarctic Circumpolar Current (ACC) and implicated as the main causal mechanism for Antarctic glaciation (Kennett, 1978; Nelson and Cooke, 2001; Houben et al., 2013). Improved understanding of the timing of major changes in the early Cenozoic evolution of the Southern Ocean will help to resolve the relative importance and inter-relationships between tectonism, biological evolution and long-term trends in atmospheric CO₂ concentration.

In this paper, we document variation in radiolarian assemblages and foraminiferal oxygen and carbon stable isotopes from the middle Eocene-to-early Oligocene interval (~ 40 to 33 Ma) at DSDP Site 277 and relate these variations to radiolarian assemblage changes at DSDP Sites 280, 281, 283 and to a previously published study of Eocene radiolarian assemblages from ODP Site 1172 (Suzuki et al., 2009). DSDP Site 277 provides a unique record of pelagic sedimentation in the Southwest Pacific from the late Paleocene to Oligocene times and the first Eocene benthic $\delta^{18}\text{O}$ record was

Expansion and diversification of high-latitude radiolarian assemblages

K. M. Pascher et al.

[Title Page](#)[Abstract](#)[Introduction](#)[Conclusions](#)[References](#)[Tables](#)[Figures](#)[◀](#)[▶](#)[◀](#)[▶](#)[Back](#)[Close](#)[Full Screen / Esc](#)[Printer-friendly Version](#)[Interactive Discussion](#)

and major events such as the MECO (~ 40 Ma) and PrOM event (~ 37.3 Ma) can be identified in the benthic $\delta^{18}\text{O}$ and $\delta^{13}\text{C}$ isotope profiles and compared to the middle Eocene-to-early Oligocene benthic isotope stratigraphy from ODP Site 689 (Diester-Haass and Zahn, 1996) (Fig. 2). The EOT is expressed as a large ($\sim 1\%$) positive shift in benthic oxygen and carbon isotopes between Cores 277-20R and -19R (Shackleton and Kennett, 1975; Keigwin, 1980), which is slightly lower than the full magnitude of the benthic $\delta^{18}\text{O}$ shift seen at other Southern Ocean sites on the Kerguelen Plateau and Maud Rise (Diester-Haass and Zahn, 1996; Zachos et al., 1996; Bohaty et al., 2012).

Foraminiferal $\delta^{18}\text{O}$ values show a normal planktic–benthic gradient with more positive values in the benthic foraminifers compared to bulk and planktic foraminifera with some crossover in the latter two (Fig. 3). Foraminiferal $\delta^{13}\text{C}$ values also show a typical positive benthic–planktic gradient. Therefore, we interpret relatively robust stable isotope signals representative of deep (intermediate), upper (thermocline) and uppermost (mixed/surface) waters, although it is likely that the $\delta^{18}\text{O}$ gradients are attenuated by diagenetic effects on planktic foraminifera (Sexton et al., 2006) as they show a “frosty” preservation.

Several short-lived climatic events are identified in the benthic stable isotope records at Site 277 (Fig. 3). The body of the MECO was not recovered (due to a 16 m sampling gap between the top of Core 277-33R and the base of Core 277-32R), but its onset and recovery is well constrained by a 0.5% negative excursion in benthic $\delta^{18}\text{O}$ values at ~ 313 mbsf (between Samples 277-33R-2, 106–108 cm and -33R-1, 129–130.5 cm) and a $\sim 0.4\%$ positive excursion in $\delta^{18}\text{O}$ values at ~ 296 mbsf (between samples 32R-3, 107–109 cm and 32R-3, 77–79 cm), indicating that the MECO spans ~ 17 m. The MECO is more strongly expressed in the benthic $\delta^{18}\text{O}$ than in the planktic record but this may relate to the poor recovery of the body of the event at this site or diagenetic impacts on planktic $\delta^{18}\text{O}$ values (Pearson et al., 2000; Sexton et al., 2006). In agreement with other records (Bohaty and Zachos, 2003; Bohaty et al., 2009), a positive $\delta^{13}\text{C}$ excursion is observed at the onset of the MECO in the benthic and bulk carbon-

ate records, although the $\delta^{13}\text{C}$ record is also compromised by the missing core of the event.

The PrOM event (Scher et al., 2014) is well-defined in the $\delta^{18}\text{O}$ record from DSDP Site 277 but also spans two significant recovery gaps between the base of Cores 277-26R, 25R and 24R (~ 244.5 to 225.5 mbsf) (Fig. 3). The $\sim 0.4\%$ positive shift in $\delta^{18}\text{O}$ that marks the onset of the PrOM, spans upper Core 277-26R and lower Core 277-25R (~ 240 – 230 mbsf), and is followed by an interval of relatively low $\delta^{18}\text{O}$ values in upper Core 277-25R, prior to reaching maximum values in uppermost Core 277-25R (~ 226 m). A gradual decrease in $\delta^{18}\text{O}$ occurs through Core 277-24R. We define the PrOM at DSDP Site 277 as the interval within these three cores in which benthic $\delta^{18}\text{O}$ exceeds 1.25% , with the exception of the interval noted above in upper Core 277-25R. These benthic $\delta^{18}\text{O}$ values are lower than those reported by Scher et al. (2014), but it is likely that peak $\delta^{18}\text{O}$ values are not captured at Site 277. Consequently the PrOM is placed between 240.62 and 219.57 mbsf (spanning a ~ 21 m section). The planktic $\delta^{18}\text{O}$ record is similar to the benthic, but lacks the maximum excursion in uppermost Core 277-25R. At the onset of the event, short-lived negative $\delta^{13}\text{C}$ excursions are evident in the benthic, bulk and planktic records. However, a longer-term positive trend for planktic and benthic $\delta^{13}\text{C}$ values becomes apparent simultaneously to the benthic $\delta^{18}\text{O}$ maximum.

Directly above the PrOM event, $\delta^{18}\text{O}$ values decrease by $\sim 0.5\%$ in upper Core 277-24R and -23R (217.37 to 207.41 mbsf), evident in benthic and planktic foraminifera as well as bulk carbonate. This interval can be correlated to the late Eocene warming interval interpreted at ODP Sites 689 (Maud Rise), 738, 744, and 748 (Kerguelen Plateau) (Diester-Haass and Zahn, 1996; Bohaty and Zachos, 2003; Villa et al., 2008, 2014).

The large positive shift in $\delta^{18}\text{O}$ defines the E-O transition at Site 277 between the base of Core 277-20R and Core 277-19R, with the most positive values in benthic and planktic $\delta^{18}\text{O}$ and $\delta^{13}\text{C}$ occurring in Core 277-19R (171.28 to 169.65 mbsf), within the earliest Oligocene.

Expansion and diversification of high-latitude radiolarian assemblages

K. M. Pascher et al.

Title Page

Abstract

Introduction

Conclusions

References

Tables

Figures

◀

▶

◀

▶

Back

Close

Full Screen / Esc

Printer-friendly Version

Interactive Discussion



4.2 Radiolarian assemblages at DSDP Site 277

In total, 16 families, 56 genera and 98 radiolarian species were identified at DSDP Site 277. Radiolarian abundance is generally low ($10\text{--}100\text{ specimens g}^{-1}$) and preservation is moderate throughout the middle Eocene-to-early late Eocene interval (349.2 to 227.2 mbsf) (Fig. 4). In the latest Eocene and early Oligocene radiolarians are abundant to very abundant ($> 1500\text{ specimens g}^{-1}$) and well preserved. Diversity is strongly correlated to abundance, which is lower in the middle and early late Eocene and high thereafter (Fig. 4). Simpson Evenness is strongly correlated to diversity but exhibits greater troughs where samples are sparse (Fig. 4). Spumellarians are dominant in most samples ranging between ~ 45 and 96% ($\sim 70\%$ average). The main families are the Actinommidae, Litheliidae, Artostrobiidae, Spongodiscidae, Lophocyrtiidae and Lychnocaniidae (Supplement Table Site 277).

Three samples from the middle Eocene (313.5, 312.7, 296 mbsf; Cores 277-32R and -33R) that lie within the onset and recovery of the MECO at Site 277, show improved preservation, a peak in diversity, and mark the first significant occurrence of diatoms (Fig. 4). The low-latitude species *Amphymenium murrayanum* and *Amphycraspedum prolixum* gr. have short-lived occurrences in this interval, with only *A. prolixum* gr. also very rare in the latest Eocene. Several species are restricted to the MECO: *Artobotrys titanothericeraos*, *Sethocyrtis chrysalis*, *Eusyringium fistuligerum* and *Stichopilium* cf. *bicorne*. *Lophocyrtis jacchia hapsis*, which is a high-latitude variant of *L. jacchia jacchia* (Sanfilippo and Caulet, 1998) and endemic to the Southern Ocean, is also common during the MECO, but is absent from the remaining middle Eocene and very rare in the late Eocene. Furthermore, the LOs of several species are recorded (albeit very rare) at this site during the MECO interval (*Axoprunum pierinae*, *Zealithapium mitra*, *Periphaena* spp., *Larcopyle hayesi*, *L. polyacantha*, *Zygocircus buetschli*, *Siphocampe?* *amygdala*, *Eucyrtidium ventriosum*, *Lychnocanium amphitrite*, *Clinorhabdus anantomus*, *Lophocyrtis kraspera*, *Lophocyrtis dumitricai*, *Cryptocarpium ornatum* and *Lamprocyclas particollis*) (Fig. 2 and Supplement Table Site 277).

era *Lithomelissa* (7) and *Larcopyle* (5) are present, as well as a higher abundance of Lophocyrtiidae. Lychnocaniids are very rare at this site (< 1 %) and the genus *Lychnocanium* is absent (Supplement Table Site 280).

4.3.2 DSDP Site 281

5 Seven samples were investigated from DSDP Site 281 in the interval between 149 and 122.5 mbsf (Cores 16R to 14R) (Fig. 5). Results from three of these samples were previously reported in Crouch and Hollis (1996) but have been re-examined for this study. Due to the presence of *Eucyrtidium spinosum* and *Eucyrtidium nishimurae*, the latter with a HO in the late Eocene at ~ 36.9–36.7 Ma (Funakawa and Nishi, 2005), we correlate the Site 281 study interval with lower Zone RP14 (~ Kaiatan local stage). A hiatus spanning the latest Eocene and Oligocene is inferred from the presence of abundant glauconite in the upper part of Core 281-14R as well as from common *Cyrtocapsella tetrapera* in Core 281-13R, which indicates a Miocene age (Crouch and Hollis, 1996).

15 In total, 14 families, 34 genera and 46 species were identified at Site 281. Radiolarians are abundant (2000–4000 specimens g⁻¹) and well preserved. Diversity is lower than at Site 280A, but Evenness is still very high and similar to the other sites (Fig. 5). The D/R ratio is very high and comparable to Site 280, except in the upper two samples in Core 281-14R (125.5–122.5 mbsf). The radiolarian assemblages are dominated by spumellarians (55–93 %), with Litheliidae (17–42 %), Spongodiscidae (12–30 %) and Actinommidae (10–0 %) the most abundant families. The most common nassellarians belong to the Plagiacanthidae (1–15 %), Lophocyrtiidae (3–7 %) and Eucyrtiidae (1–7 %) (Supplement Table Site 281). Although Sites 280 and 281 were relatively close to each other (Fig. 1), the radiolarian assemblages are distinctly different, indicating different oceanographic conditions. Crouch and Hollis (1996) concluded that Site 281 was shallower and closer to terrigenous influx than Site 280. The depositional environment of Site 280 is interpreted as more oceanic. The greater abundance of Spongodiscidae at Site 281 supports a shallower oceanic setting for this locality (Casey, 1993). Compared to the early late Eocene assemblage of Site 277, where radiolarian abundance

Expansion and diversification of high-latitude radiolarian assemblages

K. M. Pascher et al.

Title Page

Abstract

Introduction

Conclusions

References

Tables

Figures

◀

▶

◀

▶

Back

Close

Full Screen / Esc

Printer-friendly Version

Interactive Discussion



and diversity is very low, with several samples containing less than ~ 100 specimens, Site 281 contains more Spongidiscidae ($\sim 20\%$), Plagiacanthiidae ($\sim 7\%$) and Litheliidae ($\sim 20\%$), whereas the genus *Lychnocanium* is absent at Site 281.

4.3.3 DSDP Site 283

5 Six samples were examined from Site 283 between 192.25 and 87.75 mbsf (Cores 8R to 5R) (Fig. 5). The lowermost sample at 192.25 mbsf is correlated to RP13 due to the absence of *Eucyrtidium spinosum*. The uppermost five samples are of early late Eocene age based on the presence of *E. spinosum* and nannofossil age control (Edwards and Perch-Nielsen, 1975). The age of the Site 281 and 283 successions are
10 poorly defined and the PrOM event cannot be located at these sites. Both sites contain *Eucyrtidium nishimurae*: at Site 283 in all samples, at Site 281 its HO is in 125.5–122.5 mbsf. According to Funakawa and Nishi (2005) its HO is in C17n1n (~ 36.7 Ma, Gradstein et al., 2012). *E. nishimurae* is absent at Site 277. The deposition of siliceous ooze in the late middle to late Eocene and the absence (or very rare) occurrence of foraminifera suggests a deep oceanic setting close or below the Calcite Compensation
15 Depth (CCD) for Site 283.

A total of 16 families, 50 genera and 81 radiolarian species were recorded at Site 283. Radiolarians are abundant ($4700\text{--}21\,150$ radiolarians g^{-1}), with the highest abundance in Cores 283-6R and 5R, well preserved, and diverse (59–77 taxa per sample, Fisher α Index of 10–13, Evenness of 0.75–0.89). Diatoms are present in low
20 abundance with D/R ratios < 1 (Fig. 5). Spumellarians account for 59–87% of the assemblage, with the Litheliidae (23–38%), Actinommidae (5–19%) and the Spongodiscidae (2–8%) the most abundant families. The Trissocyclidae (2–11%), Eucyrtiidae (2–11%), Lophocyrtiidae (3–8%) and Plagiacanthidae (2–8%) are the most common nassellarian families (Supplement Table Site 283). *Theocyrtis tuberosa* is very abundant in the uppermost sample. The acme of this taxon might be correlated to its rare occurrence at Site 277 in the late Eocene. Several taxa appear earlier at Site 283 than
25 at Site 277. These include the following taxa that occur in the late middle Eocene (e.g.

Expansion and diversification of high-latitude radiolarian assemblages

K. M. Pascher et al.

Title Page

Abstract

Introduction

Conclusions

References

Tables

Figures



Back

Close

Full Screen / Esc

Printer-friendly Version

Interactive Discussion



Expansion and diversification of high-latitude radiolarian assemblages

K. M. Pascher et al.

Title Page

Abstract

Introduction

Conclusions

References

Tables

Figures

◀

▶

◀

▶

Back

Close

Full Screen / Esc

Printer-friendly Version

Interactive Discussion

Axoprunum bispiculum, *Amphicentria* sp. 1 sensu Suzuki, *Ceratocyrtis* spp., *Lithomelissa ehrenbergi*, *L. cf. haeckeli*, *L. sphaerocephalis*, *L. tricornis*, *Pseudodictyophimus gracilipes* gr., *Tripodiscinus clavipes*, *Siphocampe nodosaria*, *Spirocyrtis joides*, *Aspis* sp. A sensu Hollis, *Clathrocyclas universa*, *Eurystomoskevos petrushevskaae*, *Lychnocanium waiareka*, *Aphetocyrtis gnomabax*) or early late Eocene (*Spirocyrtis greeni*, *Eurystomoskevos cauleti*, *Lophocyrtis jacchia hapsis*, *Lamprocyclas particollis*) at Site 283.

4.3.4 ODP Site 1172

Forty samples were considered from ODP Site 1172 spanning a middle Eocene-to-lower Oligocene interval. Four samples from Hole D, Core 2R (356.875–355.675 mbsf) and thirty-six from Hole A, Core 48X to 39X (445.01–354.625 mbsf). The faunal assemblages of ODP Site 1172 were described by Suzuki et al. (2009), who did not correlate them to RP Zones. We identified key radiolarian index species and correlated the interval to RP Zones 10–15. The absolute age of the succession is based on the age-depth plot of Site 1172 by Stickley et al. (2004). Many taxa used to define RP zones at Site 277 are absent at Site 1172 or have diachronous ranges. We place the base of Zone RP10–12 (LO of *Theocampe mongolfieri*) at 450.55–445.01 mbsf (43.14–42.79 Ma). The base of Zone RP13 (LO of *Eusyringium fistuligerum*) can be located at 419.21–417.71 mbsf (40.48–40.35 Ma), however *Zealithapium mitra* is absent. *Eucyrtidium spinosum*, the marker for Zone RP14, has its LO at 373.75–371.21 mbsf (38.05–37.2 Ma) and *Lithomelissa tricornis* and *Pseudodictyophimus gracilipes* are absent. *Eucyrtidium antiquum* has a single LO at 365.21 mbsf (35.15 Ma), but is absent in the early Oligocene. *E. nishimurae* is present within the middle and late Eocene. Diversity and Evenness are very high throughout the succession.

Spumellarians dominate the Site 1172 assemblages throughout the middle Eocene to early Oligocene (~ 80 %). The Litheliidae are the most abundant family comprising about 20 % on average in the middle Eocene, 35 % in the late Eocene, and 25 % in the early Oligocene.

Expansion and diversification of high-latitude radiolarian assemblages

K. M. Pascher et al.

Title Page

Abstract

Introduction

Conclusions

References

Tables

Figures

◀

▶

◀

▶

Back

Close

Full Screen / Esc

Printer-friendly Version

Interactive Discussion

ter (Fig. 6), and the radiolarian diversification during the PrOM event is marked by an increase *Lithomelissa* spp. *Amphycraspedum prolixum* gr. has a trace occurrence in the latest Eocene. During the early Oligocene, overall diversity declines and especially the delicate plagiacanthiids and lophocyrtiids decrease. *Lithelius minor* gr. becomes dominant until ~ 144 mbsf, then this group decreases and high-latitude actinommid *Axoprunum bispiculum* and *A. irregularis* make up $\sim 75\%$ of the assemblage (Fig. 6).

At Sites 1172 and 283, high-latitude taxa are present from the middle Eocene, comprising 20–30% of the assemblage at Site 1172 and $\sim 40\%$ at Site 283 (Fig. 7). The MECO at Site 1172 corresponds to a decline in high-latitude taxa and an increase in cosmopolitan taxa. In the early late Eocene (~ 38 – 37 Ma), high-latitude taxa increase at Site 1172, from ~ 30 to $\sim 50\%$. High-latitude taxa at Site 281 range between 20 and 40% in the early late Eocene. At Site 283 high-latitude taxa are more abundant ranging between 40 and 55%. However, this is mainly due to the high abundance of a single taxon, *Lithelius minor* gr. Several taxa that are present in the early Oligocene at Site 280 are absent at Site 277, including *Lithomelissa challengerae*, *Larcopyle frakesi*, *Lithomelissa sakai*, and *Antarctissa* spp. The percentage of high-latitude taxa at Site 280 is between 45 and 55%, with *Lithelius minor* gr. of 10–20%. *Amphycraspedum prolixum* gr. has a trace occurrence at ~ 103 mbsf at Site 280.

5 Discussion

5.1 Comparison with geochemical temperature proxies

The radiolarian assemblages documented at Site 277 and 1172 within the MECO interval lack typical tropical taxa such as *Thyrsoyrtis* spp. (e.g. Kamikuri et al., 2013), and the low-latitude taxa *Amphycraspedum murrayanum* and *A. prolixum* gr. account for only 5% of the total assemblage at Site 277 and are absent at Site 1172. The persistence of high-latitude taxa and the variety of cosmopolitan species at both sites suggests a warm-temperate climate of ~ 15 – 20°C , in contrast to geochemical proxies

suggesting $> 25^{\circ}\text{C}$ for the MECO at Site 1172 (Bijl et al., 2010) and $\sim 27^{\circ}\text{C}$ for the late Eocene at Site 277 (Liu et al., 2009).

5.2 Nature of the Antarctic assemblage

High-latitude taxa existed from at least the middle Eocene at sites 277, 283 and 1172. Many taxa that are present from the earliest late Eocene (~ 38 Ma) at Sites 281 and 283 appear later at Site 277 ($\sim 37\text{--}36$ Ma), during the PrOM event. This appearance coincides with an increase in radiolarian abundance, diversity and preservation. A comparison of all high-latitude groups is shown in Table 2. We assigned all *Lithomelissa* spp. and *Larcopyle* spp. to the high-latitude group as they are more abundant at higher-latitude sites. The ecological and biogeographic affinity of *Lithelius minor* gr. is not yet fully understood. This group has a cosmopolitan distribution but tends to be most abundant at high-latitude sites. The sudden appearance of *Lithomelissa* spp., other high-latitude taxa and diatoms at Site 277 indicates the expansion of high-latitude water masses across the southern Campbell Plateau during the PrOM event.

5.3 High-latitude cooling and eutrophication during the PrOM event

5.3.1 Diagenesis

One possibility is that the pronounced increase in radiolarian abundance and diversity observed in the Late Eocene of Site 277 is an artefact of biogenic opal diagenesis. Chert nodules are recorded throughout the upper Paleocene-to-middle Eocene section of the cored sequence at Site 277, with a transition between chert-bearing nannofossil chalk and overlying nannofossil recorded at 246 mbsf (early late Eocene) (Kennett et al., 1975). The presence of chert combined with the generally poorer preservation of radiolarians in the lower Paleogene interval indicates some degree of diagenesis. However, the radiolarian turnover event occurs ~ 20 m above the lithological transition within the succession of nannofossil oozes, which implies that the event represents

Expansion and diversification of high-latitude radiolarian assemblages

K. M. Pascher et al.

Title Page

Abstract

Introduction

Conclusions

References

Tables

Figures

◀

▶

◀

▶

Back

Close

Full Screen / Esc

Printer-friendly Version

Interactive Discussion



Expansion and diversification of high-latitude radiolarian assemblages

K. M. Pascher et al.

Title Page

Abstract

Introduction

Conclusions

References

Tables

Figures

◀

▶

◀

▶

Back

Close

Full Screen / Esc

Printer-friendly Version

Interactive Discussion

increase in diversity, abundance and preservation of radiolarians occurs in conjunction with this event. It is also accompanied by a pronounced increase in the abundance of diatoms. Many high-latitude taxa that are very abundant at Site 281 and 283 in the late middle Eocene and early late Eocene become abundant or have their LOs at Site 277 at ~ 37 Ma, respectively: *Lithelius minor* gr., *Larcopyle hayesi*, *L. polyacantha*, *Spongopyle osculosa*, *Lithomelissa sphaerocephalis*, *L. gelasinus*, *L. ehrenbergi*, *Ceratocyrtis* spp., *Dictyophimus* aff. *archipilium*, *Lamprocyclas particollis*, and Antarctic morphotypes of *Aphetocyrtis gnomabax*, *A. rossi*, *Lophocyrtis aspera*, *L. kraspera* and *L. longiventer*. This northward extension of high-latitude taxa on the Campbell Plateau appears to have been triggered by the PrOM event, which is inferred to have been a short-lived expansion of the Antarctic ice sheet. Through the EOT, radiolarians remain abundant at Site 277, but decline in diversity. Delicate forms such as Plagiacanthidae decline, whereas *Lithelius minor* gr. and Actinommididae became dominant. The disappearance of diatoms indicates that conditions over the Campbell Plateau became nutrient-depleted. We infer that the Tasmanian Gateway was fully open by the earliest Oligocene and a strong circumpolar current was established causing widespread non-deposition in the Southwest Pacific. At the same time, a proto-Subantarctic Front developed supplying nutrient-depleted Subantarctic waters onto the Campbell Plateau resulting in a decline in radiolarian and diatom productivity.

The Supplement related to this article is available online at doi:10.5194/cpd-11-2977-2015-supplement.

Acknowledgements. This study has used bulk material and reference slides stored in the DSDP/ODP Micropaleontology Reference Centre, which is located at the Institute of Geological and Nuclear Sciences, Lower Hutt, New Zealand. We thank Noritoshi Suzuki (Tohoku University, Japan) for providing unpublished radiolarian data for ODP Site 1172. We acknowledge the support of Hannu Seebeck (GNS Science) in generating the paleogeographic maps. This project is funded by the New Zealand Marsden Fund (Contract GNS1201).

References

- Barron, J. A., Stickley, C. E., and Bukry, D.: Paleoceanographic, and paleoclimatic constraints on the global Eocene diatom and silicoflagellate record, *Palaeogeogr. Palaeoclimatol.*, 422, 85–100, 2015.
- 5 Bijl, P. K., Houben, A. J., Schouten, S., Bohaty, S. M., Sluijs, A., Reichart, G.-J., Damsté, J. S. S., and Brinkhuis, H.: Transient Middle Eocene atmospheric CO₂ and temperature variations, *Science*, 330, 819–821, 2010.
- Bijl, P. K., Bendle, J. A., Bohaty, S. M., Pross, J., Schouten, S., Tauxe, L., Stickley, C. E., McKay, R. M., Röhl, U., and Olney, M.: Eocene cooling linked to early flow across the Tasmanian Gateway, *P. Natl. Acad. Sci. USA*, 110, 9645–9650, 2013.
- 10 Bohaty, S. M. and Zachos, J. C.: Significant Southern Ocean warming event in the late middle Eocene, *Geology*, 31, 1017–1020, 2003.
- Bohaty, S. M., Zachos, J. C., Florindo, F., and Delaney, M. L.: Coupled greenhouse warming and deep-sea acidification in the middle Eocene, *Paleoceanography*, 24, PA2207, doi:10.1029/2008PA001676, 2009.
- 15 Bohaty, S. M., Zachos, J. C., and Delaney, M. L.: Foraminiferal Mg/Ca evidence for Southern Ocean cooling across the Eocene–Oligocene transition, *Earth Planet. Sc. Lett.*, 317, 251–261, 2012.
- Casey, R. E.: Radiolaria, in: *Fossil Prokaryotes and Protists*, edited by: Lipps, J. H., Blackwell Scientific Publications, Oxford/London, UK, 249–284, 1993.
- 20 Caulet, J. P.: Radiolarians from the Kerguelen Plateau, Leg 119, in: *Proceedings ODP, Scientific Results*, edited by: Barron, J. A., Larsen, B. et al., 119, Ocean Drilling Program, College Station, TX, 513–546, 1991.
- Chen, P. H.: Antarctic radiolaria, in: *Initial Reports of the Deep Sea Drilling Project*, edited by: Hayes, D. E., Frakes, L. A., et al., vol. 28, U.S. Government Printing Office, Washington, D.C., 437–513, 1975.
- 25 Crouch, E. M. and Hollis, C. J.: Paleogene palynomorph and radiolarian biostratigraphy of DSDP Leg 29, sites 280 and 281 South Tasman Rise, Institute of Geological and Nuclear Sciences science report 96/19, 46p., 1996.
- 30 Diester-Haass, L. and Zahn, R.: Eocene–Oligocene transition in the Southern Ocean: history of water mass circulation and biological productivity, *Geology*, 24, 163–166, 1996.

Expansion and diversification of high-latitude radiolarian assemblages

K. M. Pascher et al.

[Title Page](#)

[Abstract](#)

[Introduction](#)

[Conclusions](#)

[References](#)

[Tables](#)

[Figures](#)



[Back](#)

[Close](#)

[Full Screen / Esc](#)

[Printer-friendly Version](#)

[Interactive Discussion](#)



Expansion and diversification of high-latitude radiolarian assemblages

K. M. Pascher et al.

[Title Page](#)

[Abstract](#)

[Introduction](#)

[Conclusions](#)

[References](#)

[Tables](#)

[Figures](#)

[◀](#)

[▶](#)

[◀](#)

[▶](#)

[Back](#)

[Close](#)

[Full Screen / Esc](#)

[Printer-friendly Version](#)

[Interactive Discussion](#)

chos, J. C.: Early Paleogene temperature history of the Southwest Pacific Ocean: reconciling proxies and models, *Earth Planet. Sc. Lett.*, 349, 53–66, doi:10.1016/j.epsl.2012.06.024, 2012.

Hornibrook, N. de B., Brazier, R. C., and Strong, C. P.: Manual of New Zealand Permian to Pleistocene foraminiferal biostratigraphy, *Paleontological bulletin/New Zealand Geological Survey*, 56, 1–175, 1989.

Houben, A. J., Bijl, P. K., Pross, J., Bohaty, S. M., Passchier, S., Stickley, C. E., Röhl, U., Sugisaki, S., Tauxe, L., and van de Fliertdt, T.: Reorganization of Southern Ocean plankton ecosystem at the onset of Antarctic glaciation, *Science*, 340, 341–344, 2013.

Huber, M. and Sloan, L. C.: Heat transport, deep waters, and thermal gradients: coupled simulation of an Eocene greenhouse climate, *Geophys. Res. Lett.*, 28, 3481–3484, 2001.

Huber, M., Brinkhuis, H., Stickley, C. E., Döös, K., Sluijs, A., Warnaar, J., Schellenberg, S. A., and Williams, G. L.: Eocene circulation of the Southern Ocean: was Antarctica kept warm by subtropical waters?, *Paleoceanography*, 19, PA4026, doi:10.1029/2004PA001014, 2004.

Jenkins, D. G.: Cenozoic planktic foraminiferal biostratigraphy of the southwestern Pacific and Tasman Sea – DSDP Leg 29, in: *Initial Reports of the Deep Sea Drilling Project*, edited by: Hayes, D. E., Frakes, L. A., et al., vol. 29, U.S. Government Printing Office, Washington, D.C., 449–467, 1975.

Kamikuri, S.-I., Moore, T. C., Lyle, M., Ogane, K., and Suzuki, N.: Early and Middle Eocene radiolarian assemblages in the eastern equatorial Pacific Ocean (IODP Leg 320 Site U1331): faunal changes and implications for paleoceanography, *Mar. Micropaleontol.*, 98, 1–13, doi:10.1016/j.marmicro.2012.09.004, 2013.

Keigwin, L.: Palaeoceanographic change in the Pacific at the Eocene–Oligocene boundary, *Nature*, 287, 722–725, 1980.

Kennett, J. P.: Cenozoic evolution of Antarctic glaciation, the circum-Antarctic Ocean, and their impact on global paleoceanography, *J. Geophys. Res.*, 82, 3843–3860, 1977.

Kennett, J. P.: The development of planktonic biogeography in the Southern Ocean during the Cenozoic, *Mar. Micropaleontol.*, 3, 301–345, 1978.

Kennett, J. P. and Exon, N. F.: Paleoceanographic evolution of the Tasmanian Seaway and its climatic implications, in: *The Cenozoic Southern Ocean: Tectonics, Sedimentation, and Climate Change Between Australia and Antarctica*, *Geoph. Monog. Series*, 151, 345–367, 2004.

Expansion and diversification of high-latitude radiolarian assemblages

K. M. Pascher et al.

[Title Page](#)

[Abstract](#)

[Introduction](#)

[Conclusions](#)

[References](#)

[Tables](#)

[Figures](#)

[◀](#)

[▶](#)

[◀](#)

[▶](#)

[Back](#)

[Close](#)

[Full Screen / Esc](#)

[Printer-friendly Version](#)

[Interactive Discussion](#)

Raine, J. I., Beu, A. G., Boyes, A. F., Campbell, H. J., Cooper, R. A., Crampton, J. S., Crundwell, M. P., Hollis, C. J., and Morgans, H. E. G.: Revised calibration of the New Zealand Geological Timescale: NZGT2015/1, GNS Science report 2012/39, GNS Science, Lower Hutt, New Zealand, 53 pp., 2015.

5 Röhl, U., Brinkhuis, H., Stickley, C. E., Fuller, M., Schellenberg, S. A., Wefer, G., and Williams, G. L.: Sea level and astronomically induced environmental changes in middle and late Eocene sediments from the East Tasman Plateau, in: *The Cenozoic Southern Ocean: Tectonics, Sedimentation, and Climate Change between Australia and Antarctica*, edited by: Exon, N. F., Kennett, J. P., and Malone, M. J., *Am. Geophys. Union, Geophys. Monogr.*, 151, 127–151, 2004.

10 Sanfilippo, A. and Caulet, J. P.: Taxonomy and evolution of Paleogene Antarctic and Tropical Lophocyrtid radiolarians, *Micropaleontology*, 44, 1–43, 1998.

Sanfilippo, A., Westberg-Smith, M. J., and Riedel, W. R.: Cenozoic radiolaria, in: *Plankton Stratigraphy: Volume 2, Radiolaria, Diatoms, Silicoflagellates, Dinoflagellates and Ichthyoliths*, edited by: Bolli, H. M., Saunders, J. B., and Perch-Nielsen, K., 631–712, 1985.

15 Scher, H. D., Bohaty, S. M., Smith, B. W., and Munn, G. H.: Isotopic interrogation of a suspected late Eocene glaciation, *Paleoceanography*, 29, 2014PA002648, doi:10.1002/2014PA002648, 2014.

20 Seton, M., Müller, R., Zahirovic, S., Gaina, C., Torsvik, T., Shephard, G., Talsma, A., Gurnis, M., Turner, M., and Maus, S.: Global continental and ocean basin reconstructions since 200 Ma, *Earth-Sci. Rev.*, 113, 212–270, 2012.

Sexton, P. F., Wilson, P. A., and Norris, R. D.: Testing the Cenozoic multisite composite $\delta^{18}\text{O}$ and $\delta^{13}\text{C}$ curves: new monospecific Eocene records from a single locality, Demerara Rise (Ocean Drilling Program Leg 207), *Paleoceanography*, 21, PA2019, doi:10.1029/2005PA001253, 2006.

25 Shackleton, N. and Kennett, J.: Paleotemperature history of the Cenozoic and the initiation of Antarctic glaciation: oxygen and carbon isotope analyses in DSDP Sites 277, 279, and 281, in: *Initial Reports of the Deep Sea Drilling Project*, edited by: Kennett, J. P., Houtz, R. E. et al., U.S. Government Printing Office, Washington, D.C., vol. 29, 743–755, 1975.

30 Spiess, V.: Cenozoic magnetostratigraphy of Leg 113 drill sites, Maud Rise, Weddell Sea, Antarctica, *Proceedings ODP, Scientific Results*, 113, Ocean Drilling Program, College Station, TX, 261–315, doi:10.2973/odp.proc.sr.113.182.1990, 1990

Expansion and diversification of high-latitude radiolarian assemblages

K. M. Pascher et al.

Title Page

Abstract

Introduction

Conclusions

References

Tables

Figures

◀

▶

◀

▶

Back

Close

Full Screen / Esc

Printer-friendly Version

Interactive Discussion

Stickley, C. E., Brinkhuis, H., Schellenberg, S. A., Sluijs, A., Röhl, U., Fuller, M., Grauert, M., Huber, M., Warnaar, J., and Williams, G. L.: Timing and nature of the deepening of the Tasmanian Gateway, *Paleoceanography*, 19, PA4027, doi:10.1029/2004PA001022, 2004.

Suzuki, N., Ogane, K., and Chiba, K.: Middle to Late Eocene polycystine radiolarians from the Site 1172, Leg 189, Southwest Pacific, *News of Osaka Micropaleontologists*, 14, 239–296, 2009.

Takemura, A.: Radiolarian Paleogene biostratigraphy in the southern Indian Ocean, Leg 120, Proceedings ODP, Scientific Results, 120, Ocean Drilling Program, College Station, TX, 735–756, doi:10.2973.odp.proc.sr.120.177, 1992.

Takemura, A. and Ling, H. Y.: Eocene and Oligocene radiolarian biostratigraphy from the Southern Ocean – correlation of ODP Legs 114 (Atlantic Ocean) and 120 (Indian Ocean), *Mar. Micropaleontol.*, 30, 97–116, 1997.

Villa, G., Fioroni, C., Pea, L., Bohaty, S., and Persico, D.: Middle Eocene–late Oligocene climate variability: calcareous nannofossil response at Kerguelen Plateau, Site 748, *Mar. Micropaleontol.*, 69, 173–192, 2008.

Vonhof, H. B., Smit, J., Brinkhuis, H., Montanari, A., and Nederbragt, A. J.: Global cooling accelerated by early late Eocene impacts?, *Geology*, 28, 687–690, 2000.

Westerhold, T., Röhl, U., Pälike, H., Wilkens, R., Wilson, P. A., and Acton, G.: Orbitally tuned timescale and astronomical forcing in the middle Eocene to early Oligocene, *Clim. Past*, 10, 955–973, doi:10.5194/cp-10-955-2014, 2014.

Zachos, J. C., Quinn, T. M., and Salamy, K. A.: High-resolution (104 years) deep-sea foraminiferal stable isotope records of the Eocene–Oligocene climate transition, *Paleoceanography*, 11, 251–266, 1996.

Zachos, J. C., Pagani, M., Sloan, L., Thomas, E., and Billups, K.: Trends, rhythms, and aberrations in global climate 65 Ma to present, *Science*, 292, 686–693, 2001.

Table 1. Summary of species encountered at sites 277, 280, 281, and 283, their biogeographic affinity (A = Antarctic, B = bipolar, L = low-latitude and C = cosmopolitan), and location on plates for selected species.

Taxa	Biogeographic affinity	Site 277	Site 280	Site 281	Site 283	Plate
<i>Actinommidae</i> sp. A sensu Hollis		x				Pl. 1, Fig. 1
<i>Amphicentria</i> sp. 1 sensu Suzuki	A	x		x	x	Pl. 2, Fig. 1
<i>Amphicraspedum murrayanum</i> Haeckel	T	x				Pl. 1, Fig. 14
<i>Amphicraspedum prolixum</i> Sanfilippo and Riedel gr.	T	x	x			Pl. 1, Figs. 15–17
<i>Amphisphaera</i> aff. <i>radiosa</i> (Ehrenberg)		x				Pl. 1, Fig. 4a and b
<i>Amphisphaera coronata</i> (Ehrenberg) gr.	C	x			x	Pl. 1, Fig. 2
<i>Amphisphaera radiosa</i> (Ehrenberg)		x				Pl. 1, Fig. 3
<i>Amphisphaera spinulosa</i> (Ehrenberg)	C	x			x	Pl. 1, Fig. 5
<i>Amphisphaera?</i> <i>megapora</i> (Ehrenberg)		x	x	x	x	Pl. 1, Fig. 6
<i>Amphyenium splendarmatum</i> Clark and Campbell	C	x	x	x	x	Pl. 1, Figs. 18 and 19
<i>Anomalocantha dentata</i> (Mast)		x	x	x	x	
<i>Antarctissa cylindrica</i> Petrushevskaya	A		x			
<i>Antarctissa robusta</i> Petrushevskaya	A		x			
<i>Aphetocyrtis bianulus</i> (O'Connor)	A	x			x	Pl. 5, Fig. 1
<i>Aphetocyrtis gnomabax</i> Sanfilippo and Caulet	A	x	x	x	x	Pl. 5, Figs. 2–7
<i>Aphetocyrtis rossi</i> Sanfilippo and Caulet	A	x	x		x	Pl. 5, Figs. 8–11
<i>Archipilium macropus</i> (Haeckel)		x			x	
<i>Artobotrys auriculaleporis</i> (Clark and Campbell)	C	x				
<i>Artobotrys titanothericeraos</i> (Clark and Campbell)		x		x		
<i>Artostrobos annulatus</i> (Bailey)	B	x			x	
<i>Artostrobos</i> cf. <i>pretabulatus</i> Petrushevskaya	A	x				Pl. 3, Fig. 13
<i>Aspis</i> sp. A sensu Hollis	A	x	x		x	Pl. 3, Figs. 14–16
<i>Axoprunum bispiculum</i> (Popofsky)	A	x			x	
<i>Axoprunum pierinae</i> (Clark and Campbell) gr.	C	x	x	x	x	Pl. 1, Figs. 10 and 11
<i>Axoprunum?</i> <i>irregularis</i> Takemura	A	x				Pl. 1, Fig. 12
<i>Botryocella?</i> sp A sensu Apel			x			Pl. 3, Figs. 1–4
<i>Buryella granulata</i> (Petrushevskaya)	A	x				
<i>Callimitra?</i> aff. <i>atavia</i> Goll		x				Pl. 2, Fig. 2
<i>Calocycloma ampulla</i> (Ehrenberg)		x				
<i>Ceratocyrtis</i> spp.	B	x	x		x	Pl. 2, Figs. 3–5
<i>Cincolopyramis circumtexta</i> (Haeckel)	C	x	x	x	x	
<i>Cladoscenum ancoratum</i> Haeckel			x		x	
<i>Clathrocyclus universa</i> Clark and Campbell	C	x		x	x	
<i>Clinorhabdus anantomus</i> Sanfilippo and Caulet	A	x			x	Pl. 5, Figs. 12 and 13
<i>Cornutella profunda</i> Ehrenberg	C	x	x	x	x	
<i>Corythomelissa adunca</i> (Sanfilippo and Riedel)					x	
<i>Cryptocarpium bussonii</i> (Carnevale) gr.	C	x	x	x	x	Pl. 5, Figs. 25a and b, 26a and b
<i>Cryptocarpium ornatum</i> (Ehrenberg)	C	x			x	
<i>Cycladophora cosma cosma</i> Lombardi and Lazarus	A		x			Pl. 3, Fig. 17
<i>Cycladophora humerus</i> (Petrushevskaya)	A		x	x	x	Pl. 3, Fig. 18
<i>Cycladophora</i> spp.	A	x		x	x	
<i>Cymaetron sinolampas</i> Caulet			x		x	

Expansion and diversification of high-latitude radiolarian assemblages

K. M. Pascher et al.

Title Page

Abstract

Introduction

Conclusions

References

Tables

Figures



Back

Close

Full Screen / Esc

Printer-friendly Version

Interactive Discussion

Expansion and diversification of high-latitude radiolarian assemblages

K. M. Pascher et al.

Title Page

Abstract

Introduction

Conclusions

References

Tables

Figures

◀

▶

◀

▶

Back

Close

Full Screen / Esc

Printer-friendly Version

Interactive Discussion

Table 1. Continued.

Taxa	Biogeographic affinity	Site 277	Site 280	Site 281	Site 283	Plate
<i>Cyrtolagena laguncula</i> Haeckel	C	x			x	
<i>Dictyophimus?</i> aff. <i>strictus</i> O'Connor			x			Pl. 4, Figs. 9 and 10
<i>Dictyophimus infabricatus</i> Nigrini	C	x				
<i>Dictyophimus?</i> aff. <i>archipilium</i> Petrushevskaya	A	x		x	x	Pl. 4, Figs. 3a, b–8
<i>Dictyophimus?</i> <i>archipilium</i> Petrushevskaya	A	x	x		x	Pl. 4, Figs. 1a and b, 2
<i>Eucyrtidium antiquum</i> Caulet	A	x	x			Pl. 3, Fig. 19
<i>Eucyrtidium mariae</i> Caulet	A	x				
<i>Eucyrtidium microporum</i> Ehrenberg					x	
<i>Eucyrtidium nishimurae</i> Takemura and Ling	A			x	x	Pl. 3, Fig. 20a and b
<i>Eucyrtidium spinosum</i> Takemura	A	x		x	x	Pl. 3, Fig. 21
<i>Eucyrtidium</i> spp.	A				x	
<i>Eucyrtidium ventriosum</i> O'Connor	A	x			x	Pl. 3, Fig. 22
<i>Eurystomoskevos cauleti</i> O'Connor	A	x	x	x	x	Pl. 3, Fig. 23a and b
<i>Eurystomoskevos petrushevskaae</i> Caulet	A	x	x	x	x	Pl. 3, Fig. 24
<i>Eusyringium fistuligerum</i> (Ehrenberg)	C	x				Pl. 3, Fig. 25
<i>Eusyringium lagena</i> (Ehrenberg)	C				x	
<i>Glycobotrys nasuta</i> (Ehrenberg) gr.	C	x	x	x	x	Pl. 3, Figs. 5–7
<i>Heliodiscus inca</i> Clark and Campbell		x			x	
<i>Lamprocyclus particollis</i> O'Connor	A	x	x	x	x	Pl. 5, Fig. 27
<i>Larcopyle</i> cf. <i>pylomaticus</i> (Riedel)	A		x	x		Pl. 1, Fig. 25a and b
<i>Larcopyle frakesi</i> (Chen)	A		x			Pl. 1, Fig. 20
<i>Larcopyle hayesi</i> (Chen)	A	x		x	x	Pl. 1, Fig. 21
<i>Larcopyle labyrinthosa</i> Lazarus	A		x			Pl. 1, Fig. 22
<i>Larcopyle polyacantha</i> (Campbell and Clark) gr.	A	x	x	x	x	Pl. 1, Figs. 23 and 24
<i>Larcopyle</i> spp.	A	x	x	x		
<i>Lithelius foremanae</i> Sanfilippo and Riedel		x				
<i>Lithelius minor</i> Jörgensen gr.	B	x	x	x	x	Pl. 1, Figs. 26–28
<i>Lithomelissa</i> cf. <i>challengerae</i> Chen	A	x				Pl. 2, Fig. 9
<i>Lithomelissa</i> cf. <i>haeckeli</i> Bütschli	A	x			x	Pl. 2, Fig. 14
<i>Lithomelissa challengerae</i> Chen	A		x			Pl. 2, Fig. 6–8
<i>Lithomelissa ehrenbergi</i> Bütschli	A	x	x	x	x	Pl. 2, Figs. 10 and 11
<i>Lithomelissa gelasinus</i> O'Connor	A	x	x	x	x	Pl. 2, Figs. 12 and 13
<i>Lithomelissa macroptera</i> Ehrenberg	A				x	Pl. 2, Fig. 15a and b
<i>Lithomelissa robusta</i> Chen	A		x		x	Pl. 2, Fig. 16
<i>Lithomelissa sphaerocephalis</i> Chen	A	x	x	x	x	Pl. 2, Fig. 17
<i>Lithomelissa</i> spp.	A	x	x	x	x	
<i>Lithomelissa tricornis</i>	A	x	x	x	x	Pl. 2, Fig. 18
<i>Lithomelissa?</i> <i>sakai</i> O'Connor	A		x			Pl. 2, Fig. 19
<i>Lophocyrtis</i> (Apoplanius) <i>aspera</i> (Ehrenberg)	A	x		x	x	Pl. 5, Figs. 14a, b–16
<i>Lophocyrtis</i> (Apoplanius) <i>keraspera</i> Sanfilippo and Caulet	A	x			x	Pl. 5, Figs. 17–19
<i>Lophocyrtis</i> (Lophocyrtis) <i>jacchia hapsis</i> Sanfilippo and Caulet	A	x			x	Pl. 5, Figs. 20–22
<i>Lophocyrtis</i> (Paralampterium) <i>dumitricai</i> Sanfilippo	C	x				
<i>Lophocyrtis</i> (Paralampterium) <i>longiventer</i> (Chen)	A		x	x	x	Pl. 5, Figs. 23 and 24
<i>Lophocyrtis</i> spp.	A				x	

Table 1. Continued.

Taxa	Biogeographic affinity	Site 277	Site 280	Site 281	Site 283	Plate
<i>Lophophaena capito</i> Ehrenberg	C	x		x	x	
<i>Lophophaena simplex</i> Funakawa			x		x	
<i>Lychnocanium</i> aff. <i>carinatum</i> Ehrenberg		x				Pl. 4, Fig. 17
<i>Lychnocanium amphitrite</i> (Foreman)	C	x			x	Pl. 4, Figs. 11a–c and 12
<i>Lychnocanium babylonis</i> (Clark and Campbell)	C	x			x	Pl. 4, Figs. 13a and b, 14
<i>Lychnocanium bellum</i> Clark and Campbell	C	x			x	Pl. 4, Figs. 15 and 16
<i>Lychnocanium conicum</i> Clark and Campbell	C	x				
<i>Lychnocanium continuum</i> Ehrenberg					x	
<i>Lychnocanium tetrapodium</i> Ehrenberg	T	x				Pl. 4, Fig. 18a and b
<i>Lychnocanium waiareka</i> O'Connor		x			x	
<i>Perichlamyidium limbatum</i> Ehrenberg			x			
<i>Periphaena decora</i> Ehrenberg	C	x	x	x	x	
<i>Periphaena heliastericus</i> (Clark and Campbell)	C	x	x	x	x	
<i>Phormocyrtis striata striata</i> Brandt	C	x				
<i>Plectodiscus circularis</i> (Clark and Campbell)	C	x	x	x	x	
<i>Pseudodictyophimus galeatus</i> Caulet	A		x			Pl. 2, Fig. 20
<i>Pseudodictyophimus gracilipes</i> (Bailey) gr.	B	x	x	x	x	Pl. 2, Figs. 21–23
<i>Pseudodictyophimus</i> spp.	A		x			Pl. 2, Figs. 24–27
<i>Pterocodon apis</i> Ehrenberg					x	Pl. 4, Figs. 19 and 20a, b
<i>Pteropilium</i> aff. <i>contiguum</i> (Ehrenberg)		x				Pl. 4, Fig. 21
<i>Saturnalis circularis</i> Haeckel					x	
<i>Sethocyrtis chrysalis</i> Sanfilippo and Blome	C	x				Pl. 3, Fig. 26a and b
<i>Siphocampe lineata</i> (Ehrenberg)	C	x				
<i>Siphocampe nodosaria</i> (Haeckel)	C	x		x	x	
<i>Siphocampe quadrata</i> (Petrushevskaya and Kozlova)	C	x		x	x	
<i>Siphocampe? acephala</i> (Ehrenberg) gr.		x		x	x	Pl. 3, Figs. 8–10
<i>Siphocampe? amygdala</i> (Shilov)	A	x			x	Pl. 3, Figs. 11 and 12
<i>Sphaeropyle tetrapila</i> (Hays)	A	x				Pl. 1, Fig. 29
<i>Spirocyrtis greeni</i> O'Connor		x		x	x	
<i>Spirocyrtis joides</i> (Petrushevskaya)	C	x	x	x	x	
<i>Spongatractus pachystylus</i> (Ehrenberg)		x				
<i>Spongodiscus craticulatus</i> (Stöhr)				x		
<i>Spongodiscus cruciferus</i> (Clark and Campbell)	C			x		
<i>Spongodiscus festivus</i> (Clark and Campbell)	C	x				
<i>Spongopyle osculosa</i> Dreyer	B	x	x	x	x	Pl. 1, Fig. 13
<i>Spongurus bilobatus</i> Clark and Campbell	C	x		x	x	
<i>Stichopilium</i> cf. <i>bicornis</i> (Haeckel)			x	x	x	Pl. 5, Figs. 28a and b, 29a and b
<i>Stylosphaera minor</i> Clark and Campbell gr.	C	x	x		x	Pl. 1, Fig. 7
<i>Theocampe amphora</i> (Haeckel)	C	x				
<i>Theocampe urceolus</i> (Haeckel)	C	x	x	x	x	
<i>Theocyrtis tuberosa</i> Riedel	C	x			x	Pl. 5, Fig. 30
<i>Thyrsocyrtis pinguisicoides</i> O'Connor	B	x			x	Pl. 3, Fig. 27
<i>Tripodiscinus clavipes</i> (Clark and Campbell)	C	x		x	x	
<i>Zealithapium mitra</i> (Ehrenberg)	C	x			x	Pl. 1, Fig. 8
<i>Zygocircus bütschli</i> Haeckel		x			x	

Expansion and diversification of high-latitude radiolarian assemblages

K. M. Pascher et al.

[Title Page](#)

[Abstract](#) | [Introduction](#)

[Conclusions](#) | [References](#)

[Tables](#) | [Figures](#)

[◀](#) | [▶](#)

[◀](#) | [▶](#)

[Back](#) | [Close](#)

[Full Screen / Esc](#)

[Printer-friendly Version](#)

[Interactive Discussion](#)



Expansion and diversification of high-latitude radiolarian assemblages

K. M. Pascher et al.

Table 2. Average of total % of high-latitude species, groups, genera and high-latitude members of families for four time slices: MECO (~ 40 Ma), middle/late Eocene (~ 39–38 Ma), late Eocene (~ 37–35 Ma) and early Oligocene (~ 33 Ma).

	Site 280	Site 281	Site 283	Site 277		E. Olig.	Site 1172			
	E. Olig.	m/l Eoc.	m/l Eoc.	MECO	m/l Eoc.		late Eoc.	MECO	m/l Eoc	late Eoc.
% total high-lat. species	49	27	48	14	9	18	40	23	26	46
<i>Lithelius minor</i> gr. %	15.0	2.1	31.5	4.2	1.9	5.3	30.7	13.7	12.4	22.0
<i>Larcopyle</i> spp. %	10.0	10.5	1.7	2.9	1.93	1.88	1.5	6.0	5.4	12.8
<i>Lithomelissa</i> spp. %	8.9	4.8	2.5	0.06	0.1	2.15	1.2	0.5	1.4	0.5
High-lat. Lophocyrtiidae %	5.6	5.6	5.0	6.2	3.8	5.5	3.60	1.0	2.8	5.3
High-lat. Eucyrtiidae %	4.9	2.7	4.8	0.1	1.0	1.2	0.2	1.4	1.9	1.5
Other high-lat. Plagiacanthidae %	3.5	0.6	1.0	0	0.1	0.34	0.25	0	0.02	0
Other high-lat. species %	1.2	0.4	1.5	1.0	0.1	2.1	2.8	0.6	1.9	4.2

Title Page

Abstract

Introduction

Conclusions

References

Tables

Figures

◀

▶

◀

▶

Back

Close

Full Screen / Esc

Printer-friendly Version

Interactive Discussion

Expansion and diversification of high-latitude radiolarian assemblages

K. M. Pascher et al.

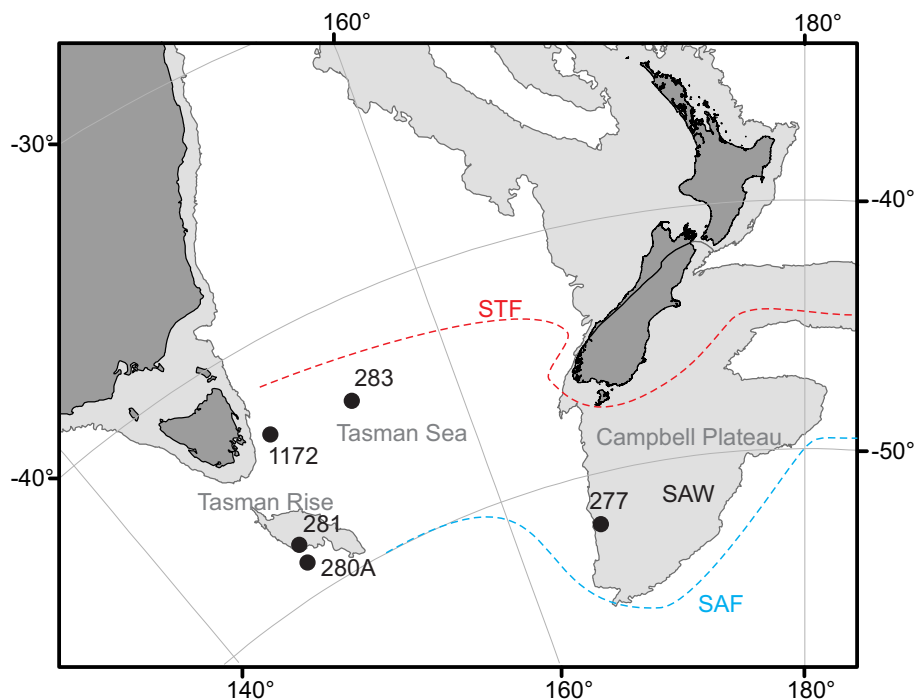


Figure 1. Modern location of DSDP and ODP study sites in the Southwest Pacific; STF = Subtropical Front, SAF = Subantarctic Front, SAW = Subantarctic Water.

[Title Page](#)

[Abstract](#)

[Introduction](#)

[Conclusions](#)

[References](#)

[Tables](#)

[Figures](#)

[◀](#)

[▶](#)

[◀](#)

[▶](#)

[Back](#)

[Close](#)

[Full Screen / Esc](#)

[Printer-friendly Version](#)

[Interactive Discussion](#)

Expansion and diversification of high-latitude radiolarian assemblages

K. M. Pascher et al.

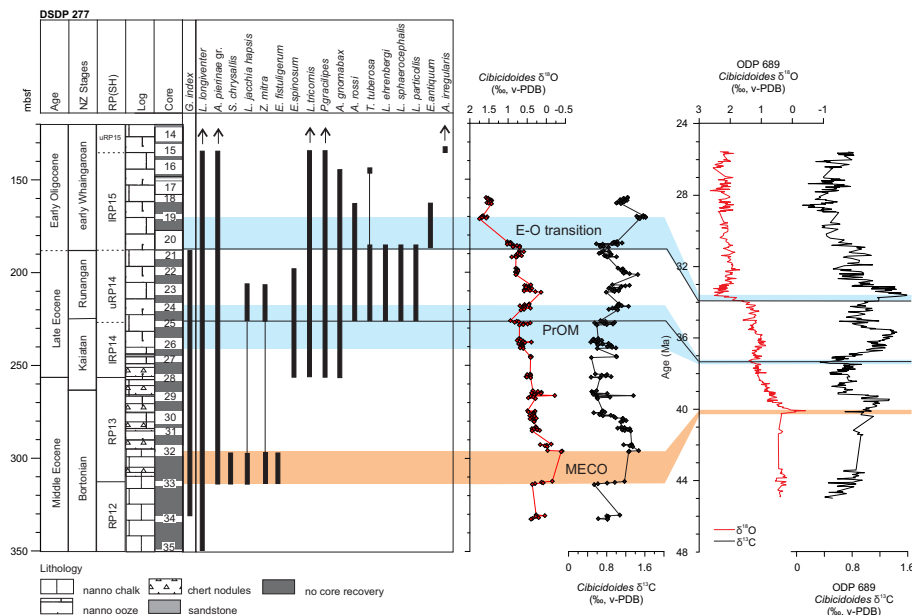


Figure 2. DSDP Site 277 stratigraphy, lithology, Southern Ocean radiolarian zones, core recovery, and ranges of *Globigerinatheka index* and selected radiolarians. Benthic stable oxygen and carbon isotope data of DSDP Site 277 correlated to Southern Ocean *Cibicidoides* data of ODP Site 689 Hole B (Maud Rise) (Diester-Haass and Zahn, 1996) calibrated to the GTS2012 timescale using the magnetostratigraphy data of Florindo and Roberts (2005) and Spiess (1990).

Title Page

Abstract

Introduction

Conclusions

References

Tables

Figures

◀

▶

◀

▶

Back

Close

Full Screen / Esc

Printer-friendly Version

Interactive Discussion

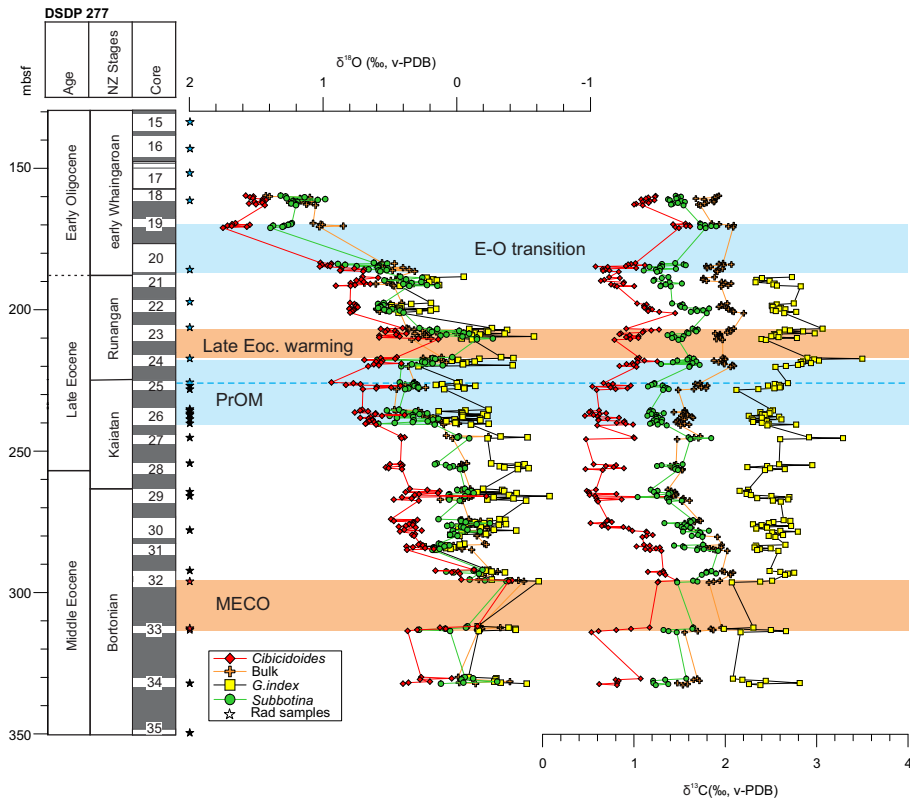


Figure 3. DSDP Site 277 oxygen and carbon stable isotope records and position of studied radiolarian samples within MECO interval (red stars) and radiolarian-rich late Eocene–Oligocene interval (blue stars).

Expansion and diversification of high-latitude radiolarian assemblages

K. M. Pascher et al.

[Title Page](#)

[Abstract](#) | [Introduction](#)

[Conclusions](#) | [References](#)

[Tables](#) | [Figures](#)

[◀](#) | [▶](#)

[◀](#) | [▶](#)

[Back](#) | [Close](#)

[Full Screen / Esc](#)

[Printer-friendly Version](#)

[Interactive Discussion](#)



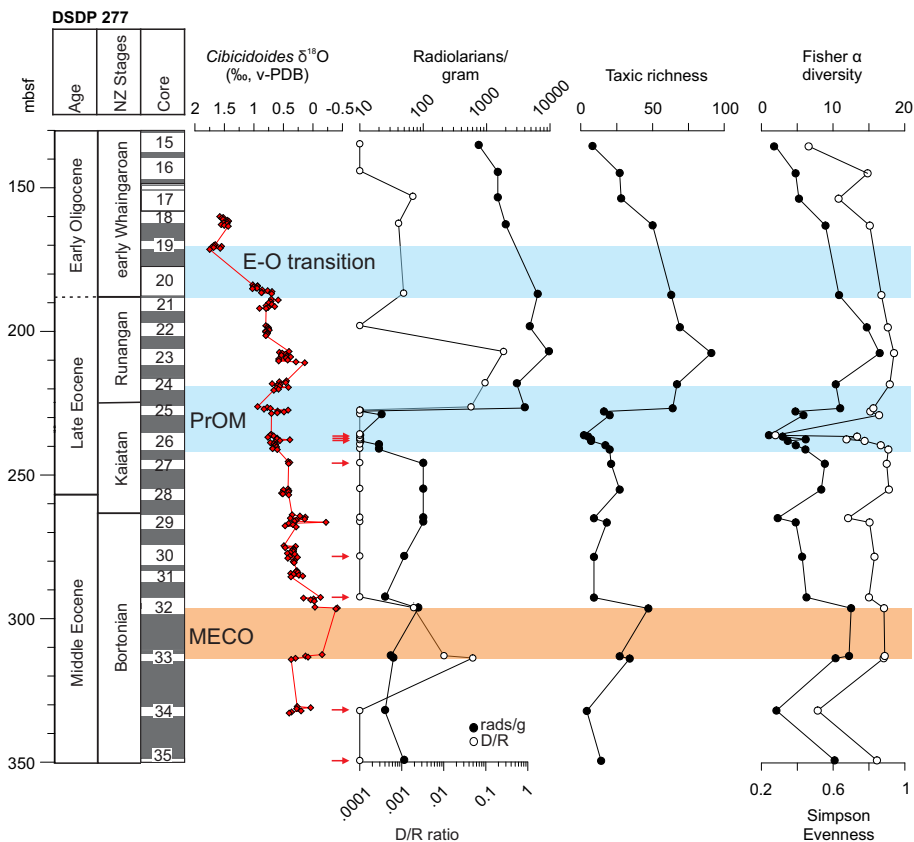


Figure 4. DSDP Site 277 benthic $\delta^{18}\text{O}$ record; radiolarian abundance and Diatom/Radiolarian (D/R) ratio; Taxic Richness (number of taxa), Fisher α Index and Simpson Evenness Index for radiolarian assemblages. Red arrows indicate samples with total specimen counts less than 99, which may be statistical insignificant but are included in all figures for the sake of completeness.

Expansion and diversification of high-latitude radiolarian assemblages

K. M. Pascher et al.

[Title Page](#)

[Abstract](#)

[Introduction](#)

[Conclusions](#)

[References](#)

[Tables](#)

[Figures](#)

[◀](#)

[▶](#)

[◀](#)

[▶](#)

[Back](#)

[Close](#)

[Full Screen / Esc](#)

[Printer-friendly Version](#)

[Interactive Discussion](#)

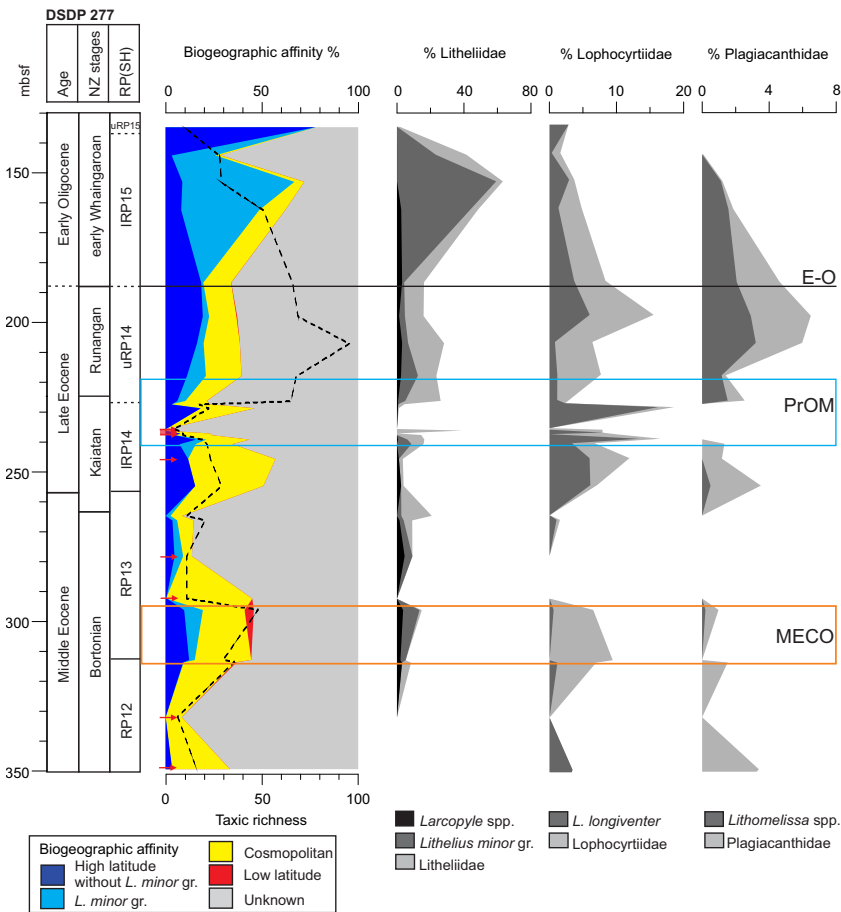


Figure 6. Biogeographic affinities of radiolarian assemblages at DSDP Site 277; Taxic richness; most abundant families with high-latitude affinity. Red arrows indicate samples with total specimen counts less than 99.

Expansion and diversification of high-latitude radiolarian assemblages

K. M. Pascher et al.

[Title Page](#)

[Abstract](#) | [Introduction](#)

[Conclusions](#) | [References](#)

[Tables](#) | [Figures](#)

[◀](#) | [▶](#)

[◀](#) | [▶](#)

[Back](#) | [Close](#)

[Full Screen / Esc](#)

[Printer-friendly Version](#)

[Interactive Discussion](#)



Expansion and diversification of high-latitude radiolarian assemblages

K. M. Pascher et al.

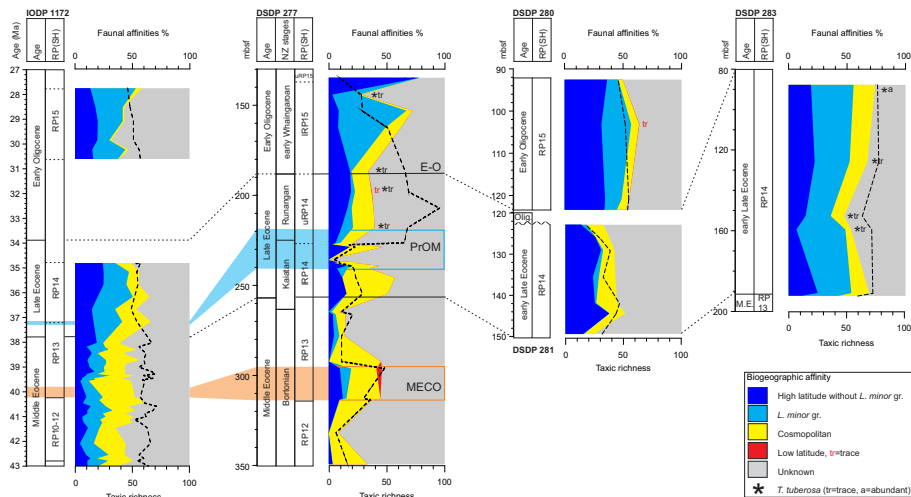


Figure 7. Variation in faunal affinities for radiolarian assemblages at all sites. Dashed black lines indicate correlation between sites, which is hampered by hiatuses and poorly defined ages, respectively. The age model of ODP Site 1172 is based on the age-depth plot of Stickley et al. (2004).

Title Page

Abstract

Introduction

Conclusions

References

Tables

Figures



Back

Close

Full Screen / Esc

Printer-friendly Version

Interactive Discussion

Expansion and diversification of high-latitude radiolarian assemblages

K. M. Pascher et al.

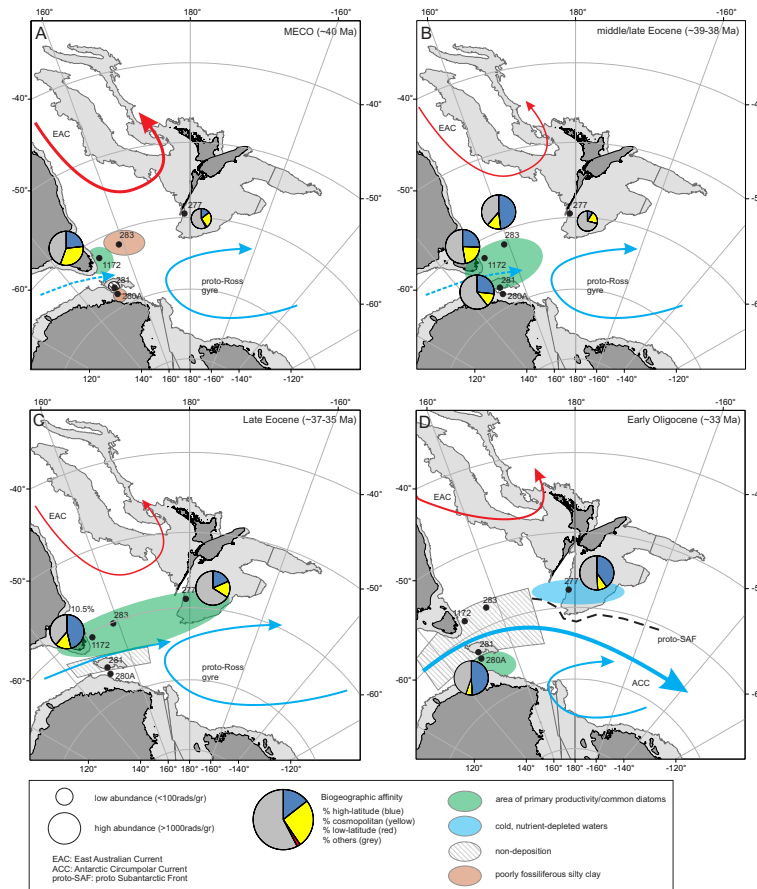


Figure 8. Paleogeographic reconstructions (GPlates, using the latest hotspot trace reference frames, Seton et al., 2012; Matthews et al., 2015) and biogeographic affinities at investigated sites during the MECO, middle/late Eocene (~ 39–38 Ma), PrOM and latest Eocene (~ 37–35 Ma) and early Oligocene (~ 33 Ma).

[Title Page](#)

[Abstract](#) | [Introduction](#)

[Conclusions](#) | [References](#)

[Tables](#) | [Figures](#)

[◀](#) | [▶](#)

[◀](#) | [▶](#)

[Back](#) | [Close](#)

[Full Screen / Esc](#)

[Printer-friendly Version](#)

[Interactive Discussion](#)